Cement & Concrete Composites 33 (2011) 319–327

Contents lists available at ScienceDirect

Cement & Concrete Composites

journal homepage: www.elsevier.com/locate/cemconcomp

Theoretical and experimental study on shear behavior of fresh mortar

Gang Lu [a], Kejin Wang [b,*]

[a] Shaw Stone & Webster, 600 Technology Center Drive, Stoughton, MA 02072, USA
[b] Iowa State University, 492 Town Engineering, Ames, IA 50011, USA

ARTICLE INFO

Article history:
Received 7 April 2009
Received in revised form 2 July 2010
Accepted 4 September 2010
Available online 21 September 2010

Keywords:
Cement paste
Mortar
Rheology
Yield stress
Friction

ABSTRACT

The shear behavior of fresh mortar is investigated using a force balance approach. In this approach, fresh mortar is considered as a two-phase material containing a matrix of cement paste and a group of rigid, spherical, non-cohesive aggregate particles. The shear resistance of a micro unit mortar is first assessed based on the friction between two contacted particles and the shear force carried by the cement paste of the micro unit mortar. The shear force of a macro-unit mortar is then calculated based on the number of the contacted aggregate particles in the mortar and the shear force carried by the rest of the cement paste. Forty-seven fresh mortar mixtures made with aggregate and paste having different characteristics and mix proportions are tested using a direct shear apparatus. The study indicates that the shear behavior of mortar follows the Mohr–Coulomb equation. The newly developed model can well predict the shear behavior of mortar materials and explain the direct shear test results.

1. Introduction

Mortar occupies over 50% of concrete volume and has significant influence on concrete properties. In the development of a concrete mix proportion, the mortar phase is often designed and evaluated first so as to select appropriate combinations of water, powder, and admixtures to take forward to concrete trial mixtures [1]. To ensure a workable concrete mixture, a layer of mortar with a sufficient thickness is required to coat the coarse aggregate particles for the mixture to have an adequate flowability. In self-consolidating concrete (SCC), mortar has to have proper deformability for the concrete mixture to achieve self-consolidation and adequate yield stress to prevent segregation of coarse aggregate [2,3]. Understanding the shear behavior of mortar is essential for designing a workable concrete mixture [4].

Two important rheological parameters are often used to describe the flow behavior of concrete materials: yield stress and viscosity. A "true" yield stress is the shear stress required by an elastic–viscous material for initiating a plastic deformation. It is the maximum shear stress under which the material keeps in a static state [5]. A material must overcome the yield stress to transform from solid to liquid behavior. The present study is to investigate the yield behavior of a fresh mortar and deals with the mortar material under a static state. Viscosity is the resistance of a material to flow, and it describes the material behavior in a dynamic state, which is not studied in the present paper.

Presently, yield stress of a concrete material is often determined by some workability tests [5–7]. The yield stresses measured from these tests are actually called Bingham yield stress, rather than the "true" yield stress. Due to variations in the test equipment and procedures, the Bingham yield stresses obtained from different experiments often vary largely [5]. Some research has been conducted studying the relationship between the "true" and Bingham yield stresses [5,7]. However, most of these studies are still based on experimental approaches. The study of the "true" yield stress of mortar is limited.

Li et al. [8] attempted to model the "true" yield stress of high flowability fresh concrete. They considered concrete as a particle assembly and assumed that the interparticle force was generated by the friction between the particles and the link resulting from the surface tension and suction of pore water. Although their model qualitatively described yield behavior of some cementitious materials, they neglected the factor that the cement particles are cohesive and aggregate particles are non-cohesive.

In the modeling of mortar/concrete flowability, the amount of excess paste that coats aggregate particles and the rheology of the paste are essential. It is the excess paste, rather than the paste that fills the voids among the aggregate particles, that maintains a mortar or concrete flow [9]. Oh et al. reported that when the thickness of the excess paste that coats aggregate particles increased, both the yield stress and viscosity of concrete decreased, thus resulting in flowable concrete [10]. For given paste content, the excess paste thickness is dependent on the aggregate gradation. Well-graded aggregate contains less volume of voids among its particles and requires less paste to fill the voids among the particles so that more paste remains and coats the aggregate particles,

* Corresponding author. Tel.: +1 515 294 2152; fax: +1 515 294 8216.
E-mail address: kejinw@iastate.edu (K. Wang).

0958-9465/$ - see front matter © 2010 Elsevier Ltd. All rights reserved.
doi:10.1016/j.cemconcomp.2010.09.002

Nomenclature

$A_{\text{cross agg}}$	cross section area on the slant plane of cement paste bridging two aggregate particles
A_p	net area of cement paste in a unit volume of mortar
C_M	cohesion of fresh mortar
D_0	the average diameter of the aggregate particles retained on a given sieve, i
D_i	the average diameter of the ith group, $D_i = \frac{(D_i)_{\max}+(D_i)_{\min}}{2}$, where $(D_i)_{\max}$ is the maximum diameter of ith group and $(D_i)_{\min}$ is the minimum diameter of ith group
f_c	shear force from cement paste, see Fig. 3
f_i	interparticle force, see Fig. 3
f_i^n	component of interparticle force (f_i) on direction normal to the local slant surface, see Fig. 3
f_i^t	component of interparticle force (f_i) on direction of the local slant surface, see Fig. 3
i	the order of the sieves used.
V_{agg}	volume fraction of aggregate in a unit volume of mortar
N_{agg}	number of aggregate particles in a unit volume of mortar
P	probability of aggregate contacting to other particles
P_1	combination parameter of probability for internal friction angle of mortar
P_2	combination parameter of probability for cohesion of mortar
S	average interparticle distance
$V_{\text{uncomp agg}}$	volume of voids among aggregate particles in a unit volume of mortar at granulate dry state
voids	un-compacted void content of the aggregate particles
V_{paste}	volume of cement paste in a unit volume of mortar
$V_{\text{excess paste}}$	volume of excess paste in a unit volume of mortar
S	average interparticle distance
α	angle of direction, see Fig. 3
β	angle of direction, see Fig. 3
σ_i	normal force applied on particle, see Fig. 4
ϕ_{agg}	friction angle of aggregate particles in dry granular state
ϕ_M	friction angle of fresh mortar
θ	local force concentrate angle, see Fig. 3
μ	friction coefficient of aggregate particles in dry granular state
τ_M	yield stress of mortar
τ_{NP}	shear stress from net paste in a unit volume of mortar
τ_{agg}	shear stress from contact aggregate particle friction in a unit volume of mortar
τ_p	yield stress of cement paste in mortar
τ_i	shear force generated by particle friction, see Fig. 3

which will contribute to the mortar/concrete flow [11,12]. Su et al. applied the excess paste theory to design SCC [13]. Coupling the excess paste thickness concept with other theoretical approaches, the authors of this paper have developed some models for predicting yield stress of a cement paste and shear stress of a mortar [14,15].

The objective of the present study is to investigate the shear behavior and "true" yield stresses of fresh mortars. In this study, the model for mortar shear behavior is developed using a force balance approach from a micro-scale to macroscale level. The interparticle distance, corresponding to the excess paste, is considered in the model. Forty-seven (47) fresh mortar mixtures made with different water-to-cement ratios (w/c), sand-to-cement ratios (s/c), and aggregate size and gradations are tested using a direct shear apparatus. These experimental results determine the values of probability parameters used in the theoretical model, through which the model is then calibrated and validated. Using the newly developed model, the shear behavior of mortar materials can be predicted and the direct shear test results can be well explained.

2. Model development

In the present model development, fresh mortar was considered as a two-phase material, which contains a matrix of cement paste and a group of rigid, spherical, non-cohesive aggregate particles (Fig. 1). The shear force of a micro-scale mortar unit, also called a micro unit, which consists of two contacted aggregate particles surrounded by a layer of cement paste, was first assessed from all forces balanced on a micro slant surface. The shear force was assumed resulting from the friction between these two contacted particles and the shear force carried by the cement paste of the micro unit. The shear force of a conventional unit volume of the mortar (such as a cubic centimeter or cubic meter of mortar), also called a macro-unit mortar, was then calculated based on the number of the contacted aggregate particles in the macro-unit and the shear force carried by the rest of cement paste. The number of the contacted aggregate particles in the macro-unit mortar was estimated based on the probability concept. The details in the shear stress model development are presented in the following sections.

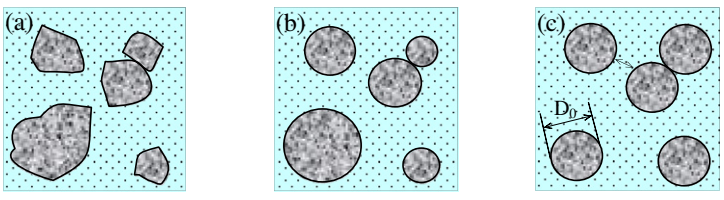

(a) a "real" mortar
(b) a simplified mortar (aggregate particles are rigid spheres)
(c) a further simplified mortar (aggregate particles are equal-sized rigid spheres, with an average diameter of D_0 and net space of S.)

Fig. 1. Simplification of fresh mortar system.

2.1. Assumption and simplification

The following assumptions were made to simplify a mortar:

1. The cement paste of the mortar is an ideal elastic–viscous material with known rheological properties.
2. All aggregate particles in the mortar are rigid, spherical, dry, and non-cohesive particles.
3. The different sizes of graded aggregate can be represented by a group of single-sized spheres with an average diameter (D_0).
4. The mortar is freshly mixed, and the cement paste properties of the mortar do not change during the short time of this rheology study. There is no bond between the cement paste and aggregate particles. No static aggregate segregation occurs in the mortar mixture.
5. No entrained or entrapped air voids exist in the mortar.

Based on the above assumptions, a macro-unit volume of an actual mortar, composed of well-graded, irregular-shaped aggregate particles in a cement paste (Fig. 1a), can be simplified as an "ideal" mortar that consists of single-sized, rigid, spherical particles in a elastic–viscous paste (Fig. 1c via Fig. 1b).

2.2. Volumetric calculations

The average diameter (D_0) of the single-sized spherical aggregate particles in Fig. 1c can be determined by Eq. (1), according to the actual aggregate gradation [16]:

$$D_0 = \left[\frac{1}{\sum p_i D_i^{-3}}\right]^{1/3} \tag{1}$$

where, D_0 is the average diameter of all aggregate particles in the mortar; p_i is volume fraction of the aggregate particles on a given sieve, and i; D_i is the average diameter of aggregate particles on sieve i;

$$D_i = \frac{(D_i)_{\max} + (D_i)_{\min}}{2}$$

where $(D_i)_{\max}$ is the maximum diameter of aggregate particles on sieve i; $(D_i)_{\min}$ is the minimum diameter of aggregate particles on sieve i; and i is the order of the sieves used.

The number of aggregate particles (N_{agg}) in a macro-unit volume of mortar having the aggregate volume fraction of V_{agg} is given by:

$$N_{\text{agg}} = \frac{V_{\text{agg}}}{\frac{4}{3}\cdot\pi\cdot\left(\frac{D_0}{2}\right)^3} = \frac{6V_{\text{agg}}}{\pi D_0^3} \tag{2}$$

The volume of void among the un-compacted aggregate particles ($V_{\text{uncomp voids}}$) in the macro-unit volume of the mortar can be obtained from the un-compacted void content of aggregate particles ($n_{\text{uncomp agg}}$) measured according to ASTM C1252 [17]:

$$V_{\text{uncomp voids}} = \frac{n_{\text{uncomp agg}}}{1 - n_{\text{uncomp agg}}}\cdot V_{\text{agg}} \tag{3}$$

The volume of cement paste (V_{paste}) in the macro-unit volume of the mortar is:

$$V_{paste} = 1 - V_{\text{agg}} \tag{4}$$

The volume of the excess cement paste ($V_{\text{excess paste}}$) is defined as the total volume of the cement paste (V_{paste}) minus the volume of cement paste that fills the voids among the aggregate ($V_{\text{paste in voids}}$), which is equal to the volume of void among the un-compacted aggregate particles ($V_{\text{uncomp voids}}$). The volume of the excess cement paste ($V_{\text{excess paste}}$) can be expressed as below [9]:

$$V_{\text{excess paste}} = V_{paste} - V_{\text{paste in voids}} = 1 - \frac{1}{1 - n_{\text{uncomp agg}}}\cdot V_{\text{agg}} \tag{5}$$

The average interparticle distance ($\bar{S}$) is defined as the average net distance between two aggregate particles, and it can be calculated from the volume of the excess cement paste in a macro-unit volume of mortar ($V_{\text{excess paste}}$), the number of aggregate particles in the mortar (N_{agg}), and the surface area of a single aggregate particle ($A_{particle} = \pi D_0^2$), as given below:

$$\bar{S} = \frac{2V_{\text{excess paste}}}{N_{\text{agg}}\cdot A_{\text{particle}}} = \frac{D_0}{3V_{\text{agg}}}\cdot\left(1 - \frac{V_{\text{agg}}}{1 - n_{\text{un-compacted agg}}}\right) \tag{6}$$

2.3. Stress analyses

Fig. 2 illustrates the mechanism by which the shear stress (τ) is generated in a given shear plane of a macro-unit volume of a freshly mixed mortar under a normal stress (σ). Based on the force balance concept, the external shear stress (τ), resulting from the applied normal stress (σ), should be balanced by the internal shear stresses of the mortar material. Two sources of the internal shear stresses are considered in the present model: (1) the friction between contacted aggregate particles and (2) the shear stress carried by the cement paste (τ_p).

In order to obtain the overall stress of the mortar, the interaction of two particles is studied first. Fig. 3a shows the forces acted on a two particle micro unit of a macro-unit of mortar. The two particles (i and j) are coated with a uniform layer of cement paste except for the contacting point C. At the contact point, a force (f_i) is generated due to the particle interaction. This internal force (f_i) can be divided into two components and serve as one source of the resistance to the normal and shear stresses (σ_i and τ_i) of the macro-unit mortar. Thus, the normal stress (σ_i) and the shear stress (τ_i) contributed by the internal force (f_i) in a micro unit mortar can be written as [14,15]:

$$\sigma_i = f_i^y = f_i\cdot\cos\alpha; \quad \text{and} \tag{7}$$

$$\tau_i = f_i^x = f_i\cdot\sin\alpha\cos\beta \tag{8}$$

where α and β are position angles of force f_i in x–y–z coordinate (see Fig. 3b).

When a number of micro units are considered in a macro-unit mortar, the average shear and normal stresses ($\bar{\tau}_i$ and $\bar{\sigma}_i$) of the micro units can be assessed based on the probability concept as shown by Eqs. (7) and (8). The probability (P_i) of the force (f_i) falling in the range of a half sphere, as illustrated in Fig. 3b, can be determined by two position angles α and β. This probability value (P_i) can be expressed as [18]:

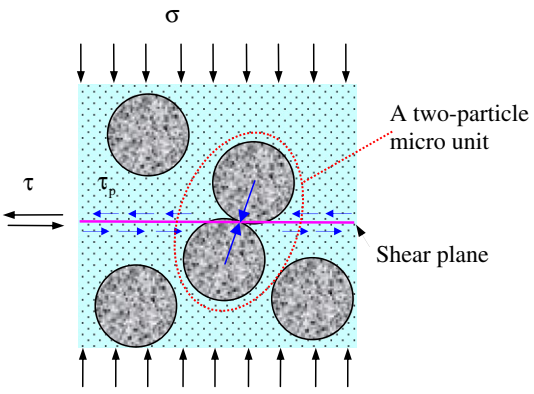

Fig. 2. Force acted on a macro-unit of mortar.

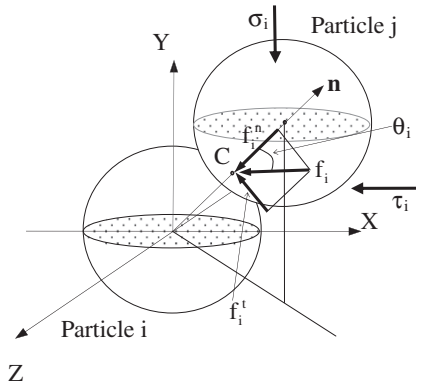

(a) Forces acted on a micro unit of mortar

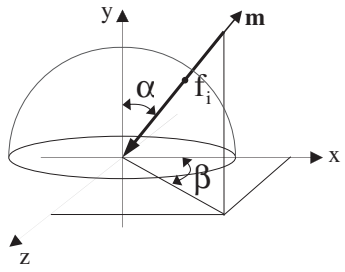

(b) Position of force f_i

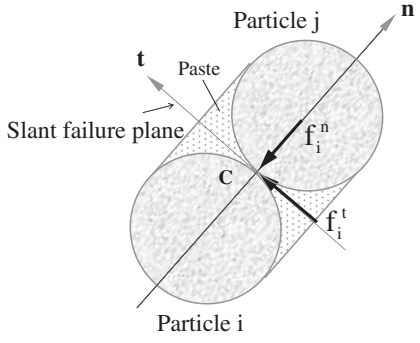

(c) Slant failure plan of the micro unit

Fig. 3. Stresses development in a micro unit of mortar.

$$P_i(\alpha,\ \beta) = \frac{\sin\alpha \cdot d\beta \cdot d\alpha}{\pi} \tag{9}$$

where, $\alpha \in \left[0\frac{\pi}{2}\right]$ and $\beta \in \left[-\frac{\pi}{2}, \frac{\pi}{2}\right]$.

Thus, the average shear and normal force of a typical micro unit can be obtained as:

$$\bar{\tau}_i = \int_{\alpha,\beta}\int \frac{\sin\alpha}{\pi} \cdot \tau_i \, d\alpha \, d\beta = 0.637 \cdot f_i \tag{10}$$

$$\bar{\sigma}_i = \int_{\alpha,\beta}\int \frac{\sin\alpha}{\pi} \cdot \alpha_i \, d\alpha \, d\beta = 0.5 \cdot f_i \tag{11}$$

Similar to that in soils, shearing strength of a fresh mortar is the result of the resistance to movement at interparticle contact. Therefore, the maximum shear of the micro unit mortar can be assumed to occur on the slant plane that goes through the two particle contacting point and is perpendicular to the center line of the two particles studied (Fig. 3c). According to Fig. 3a, the particle interaction force generated on the slant plane (f_i^t) can be determined as $f_i^t = f_i \cdot \sin\theta$, where θ is the local concentrated angle of two contact aggregate particles. This force (f_i^t) results from two sources: (1) the friction between the two contacted particles and (2) the shear force carried by the cement paste of the micro unit, and it can be expressed as:

$$F_i^t = f_i^n \cdot \mu + f_c \tag{12}$$

where, $f_i^n = f_i \cdot \cos\theta$; μ is the friction coefficient of the aggregate particles; and f_c is the shear force generated by cement paste on the slant plane. f_c can be determined as:

$$f_c = \tau_P \cdot A_{paste,m} \tag{13}$$

where, $A_{\text{paste, m}}$ is the area of the cement paste enclosed by the two aggregate particles of a micro unit and projected on the slant plane, or $A_{\text{paste, m}} = \pi D_0^2/4$.

It is noted that the form of Eq. (12) is similar to that of the Mohr–Coulomb equation, which is commonly used to express the shear failure condition of rock or soil.

Combining Eqs. (10)–(13), the following equation can be obtained:

$$\frac{\bar{\tau}_i}{0.637} \cdot \sin\theta = \frac{\bar{\sigma}_i}{0.5} \cdot \cos\theta \cdot \mu + \tau_p \cdot A_{\text{paste, m}} \tag{14}$$

Through a different study, the authors have found the correlation between aggregate particles friction angle (ϕ_{agg}) and their friction coefficient (μ) as $\tan(\phi_{agg}) = 1.274\ \mu$ [18]. Thus Eq. (14) can be rewritten as:

$$\bar{\tau}_i = \frac{\tan\phi_{\text{agg}}}{\tan\theta} \cdot \bar{\sigma}_i + \frac{0.637\tau_p \cdot A_{\text{paste, m}}}{\sin\theta} \tag{15}$$

Eq. (15) gives the average value of the shear force generated by a micro unit containing two contacted aggregate particles.

It is assumed that in a macro-unit shear plane, there are N_{agg} aggregate particles (see Eq. (2)), and the probability that these aggregate particles getting in touch is known as P. (The calculation of P value will be discussed later.) Thus, the subtotal shear stress resulting from the friction of the contacted aggregate particles in the shear plane (τ_{agg}) can be expressed as:

$$\begin{aligned}\tau_{\text{agg}} &= P \cdot N_{\text{agg}} \cdot \tau_i \\ &= P \cdot N_{\text{agg}} \cdot A_{\text{paste, m}} \left(\frac{\tan\phi_{\text{agg}}}{\tan\theta} \cdot \sigma + \frac{0.637}{\sin\theta} \cdot \tau_p\right)\end{aligned} \tag{16}$$

The shear force resulting from the net cement paste (τ_{NP}), not including the paste enclosed by the touched aggregate particles, in the macro-unit shear plane of mortar is:

$$\tau_{NP} = \tau_P \cdot A_P = (1 - P \cdot N_{\text{agg}} \cdot A_{\text{paste, m}} \cdot \cos\alpha) \cdot \tau_P \tag{17}$$

where, A_p is the net area of cement paste in a macro-unit volume of mortar. It is the area of the macro-unit shear plane subtracting the area of the paste enclosed in all micro units of contacted aggregate particles. A_p can be calculated as:

$$A_P = 1 - P \cdot N_{\text{agg}} \cdot A_{\text{paste, m}} \cdot \cos\alpha \tag{18}$$

Combining Eqs. (16)–(18), the total shear force generated in the macro-unit mortar shear plane (τ_M) becomes:

$$\begin{aligned}\tau_M = \tau_{NP} + \tau_{\text{agg}} &= (1 - 0.5 \cdot P \cdot N_{\text{agg}} \cdot A_{\text{paste, m}}) \cdot \tau_P \\ &+ P \cdot N_{\text{agg}} \cdot A_{\text{paste, m}} \left(\frac{\tan\phi_A}{\tan\theta} \cdot \sigma + \frac{0.637}{\sin\theta} \cdot \tau_p\right)\end{aligned} \tag{19}$$

Eq. (19) can be simplified as:

$$\begin{aligned}\tau_M &= \frac{3 \cdot P \cdot V_{\text{agg}}}{2 \cdot D_0 \cdot \tan\theta} \cdot \tan\phi_{\text{agg}} \cdot \sigma \\ &+ \left[1 + \left(\frac{0.9555}{\sin\theta} - 0.75\right) \cdot \frac{P \cdot V_{\text{agg}}}{D_0}\right] \cdot \tau_P\end{aligned} \tag{20}$$

$$\text{Given } \tan\phi_M = \frac{3\cdot P\cdot V_{agg}}{2\cdot D_0\cdot\tan\theta}\cdot\tan\phi_{agg} = P_1\cdot\tan\phi_{agg} \quad (21)$$

$$\text{and } C_M = \left[1+\left(\frac{0.9555}{\sin\theta}-0.75\right)\cdot\frac{P\cdot V_{agg}}{D_0}\right]\cdot\tau_P = [1+P_2]\cdot\tau_P, \quad (22)$$

Eq. (20) can be rewritten as:

$$\tau_M = \tan\phi_M\cdot\sigma + C_M \quad (23)$$

$$\text{or } \tau_M = P_1\cdot\tan\phi_{agg}\cdot\sigma + (1+P_2)\cdot\tau_P \quad (24)$$

where,

$$P_1 = \frac{3\cdot P\cdot V_{agg}}{2\cdot D_0\cdot\tan\theta} = \frac{\tan\phi_M}{\tan\phi_{agg}}$$

and

$$P_2 = \left(\frac{0.9555}{\sin\theta}-0.75\right)\cdot\frac{P\cdot V_{agg}}{D_0} = \frac{C_M}{\tau_P}-1$$

Since P_1 and P_2 containing the probability term (P), they are called probability parameters. τ_p is the yield stress of cement paste, which can be obtained from either rheology test or modeling [14].

Again, the form of Eq. (23) appears the same as that of the Mohr–Coulomb equation. Correspondingly, ϕ_M can be defined as the friction angle and C_M can be defined as the cohesion of mortar. C_M is also the yield stress under zero normal stress, or the rheological "true" yield stress of the mortar.

Based on Eqs. (23) and (24), the value of tan φ_M depends upon the aggregate characteristics (ϕ_{agg} and D_0) and volume fraction (V_{agg}), the probability that the aggregate particles in a mortar under a shear force may get in touch (P), and the local force concentrate angle (θ). As explained in the following, both θ and P depend upon the average interparticle distance (S), which also relies on aggregate characteristics and volume fraction.

The angle θ randomly varies in the range of $(0°, 90°)$. When $\theta = 90°$, a layer of excess cement paste exists between aggregate particles of the mortar (or $S > 0$), and there is no touch between the aggregate particles ($\tan\phi_M = 0$). Thus, the yield condition of fresh mortar (Eq. (23)) becomes $\tau_M = C_M$. When $\theta = 0°$, all forces applied onto two adjacent aggregate particles are coaxial with the axis connecting the gravity centers of the two particles, which is an extreme interlock situation. In this case, the mortar is not a particle assembly but a piece of solid. As a result, θ of a mortar should be larger than zero.

As discussed later, the probability parameters P_1 and P_2 can be obtained from their relationship with S through the curve fitting of test data. Like parameters V_{agg}, D_0, and S, P_1, and P_2 are also material-related parameters and dependent on the mortar mix proportion. Therefore, the quantitative predictions for the friction angle (ϕ_M) and cohesion (C_M) of mortar can still be achieved from Eqs. (23) and (24) with no need of any experimental results.

Note that Eq. (24) is a different format of Eq. (23). As discussed later, using Eq. (24), the parameters (ϕ_M and C_M) of Eq. (23) can be studied more easily.

3. Experimental work

In order to verify validity of the newly developed model and find out the effects of mortar material properties on yield stress, a group of mortar mixtures made with different w/c, s/c, and sand gradations were tested by using a direct shear test.

3.1. Materials

Type I Portland cement was used in mortar and its chemical and physical properties are shown in Table 1. No chemical admixture was employed. River sand was used as fine aggregate, and its specific gravity was 2.63 under the saturated surface dried (SSD) condition and 2.59 under the oven dried (OD) condition. Four single-sized aggregates (#16, #30, #50, and #100) and three graded aggregates (G1, G2, and G3, with fineness modulus (F.M.) of 3.40, 2.81, and 2.25 respectively) were used. G1 and G3 are the high and low limits of ASTM C33, Standard Specification for Concrete Aggregates, and G2 is in the middle of G1 and G3. The other properties of the aggregate are presented in Table 2. The un-compacted void content of the aggregates was measured according to ASTM C1252 [17], the Standard Test Method for Un-compacted Void Content of Fine Aggregate. The average diameter of the aggregates (D_0) was calculated from Eq. (1). The friction angles of the aggregates (ϕ_{agg}) were obtained from a direct shear test.

3.2. Mix proportions

Three cement pastes made with different w/c were used in mortar. Table 3 gives the yield stresses of the pastes, measured by a BROOKFIELD rheometer. Table 4 shows the mortar mix proportions with different w/c, s/c, aggregate size and gradations. In total, forty-seven (47) mortar mixtures were studied.

3.3. Mixing procedure

All cement and mortar samples were mixed according to ASTM C305 "Standard Practice for Mechanical Mixing of Hydraulic Cement Pastes and Mortars of Plastic Consistency" [19]. The temper-

Table 1
Chemical and physical properties of cement.

Oxide composition (%)	CaO	SiO_2	Al_2O_3	Fe_2O_3	MgO	SO_3
	62.96	20.96	4.54	3.48	2.91	2.77
	C_3S	C_2S	C_3A	C_4AF	Gypsum	
	53.71	19.58	6.14	10.59	0.78	
Physical properties	Specific gravity			Fineness		
	3.15			373 m^2/kg		

Table 2
Aggregates and properties.

ID	Un-compacted void content	Average diameter, D_0 (mm)	Friction angle*, ϕ_{agg} (°)
RS#16	0.420	1.770	41.03
RS#30	0.445	0.890	41.31
RS#50	0.450	0.450	41.31
RS#100	0.458	0.225	41.24
RS-G1	0.358	0.523	41.17
RS-G2	0.372	0.364	40.99
RS-G3	0.395	0.222	41.24

* The aggregate friction angle was measured from a direct shear box test. It is independent of aggregate size. Therefore, the average friction angle of the river sand ($\phi_{agg} = 41°$) is used in the present study.

Table 3
Cement pastes and properties.

Paste #	P1	P2	P3
w/c	0.35	0.40	0.45
Yield stress, τ_p (Pa)	473.6	205.2	148.4

Table 4
Mortar mix proportions.

Aggregate	Paste	*s*/*c*
#16	P1, P2, P3	1
#30	P1, P2, P3	1
#50	P1, P2, P3	1
#100	P3	1
G1	P1, P2, P3	1
G2	P1, P2, P3	1
G3	P1, P2, P3	1
#16	P1, P2, P3	2
#30	P2, P3	2
#50	P2, P3	2
#100	P3	2
G1	P1, P2, P3	2
G2	P1, P2, P3	2
G3	P1, P2, P3	2
#16	P3	3
#30	P3	3
G1	P1, P2, P3	3
G2	P1, P2, P3	3
G3	P1, P2, P3	3

ature of mixing water was controlled at 25 °C (77 °F). The environmental temperature and relative humidity were 25 ± 1.5 °C (77 ± 2.7 °F) and 36 ± 3%, respectively, during the sample mixing and the Rheometer and direct shear tests.

3.4. Direct shear test

ELE Direct/Residual Shear Apparatus for geotechnical material was used in present study. The apparatus have a round shear area, which is 3167 mm^2 (4.9089 in.^{2}). The shear rate was controlled as 1 mm/min. The total shear deformation is 5 mm (0.1969 in.). In order to prevent the leaking of cement paste in the shear box, the gaps between upper and lower shear boxes and the gaps between the loading plate and the vertical surface of upper shear box were sealed with a mineral grease. Three different normal stresses (0; 30.945; and 61.890 kPa (0; 4.488; and 8.977 psi)) were applied to the mortar samples. The whole shear test process (from the contact of the cement with water to the end of the test) is about 15 min.

4. Results and discussions

4.1. Typical direct shear test results

Fig. 4a shows the typical direct shear test results of a mortar sample (w/c = 0.35; s/c = 1, RS#30) under three different levels of normal stresses (0; 30,945; and 61,890 Pa (0; 4.488; and 8.977 psi)). It is observed in the figure that shear stress of the mortar increases with normal stress. The peak shear stress of each curve can be considered as the maximum shear resistance of the mortar under the given normal stress. As a result, the relationship between the maximum shear resistance and its normal stress of the mortar samples presented in Fig. 4a can be plotted as Fig. 4b. This relationship, approximately linear, is similar to that described by the Mohr–Coulomb equation that is commonly used to express the shear failure condition of rock and soil. Comparably, the internal friction angle (ϕ_M) of the mortar can be determined from the slope of the shear stress–normal stress curve, and the cohesion (C_M) can be determined from the intercept of the linear fitting line on shear stress axis. Based on the rheological definition, the rheological yield stress of the tested mortar is the maximum shear resistance at zero normal stress, under which the fresh mortar will not have shear deformation. This rheological yield stress from the direct shear test can be considered as the "true" yield stress of mortar.

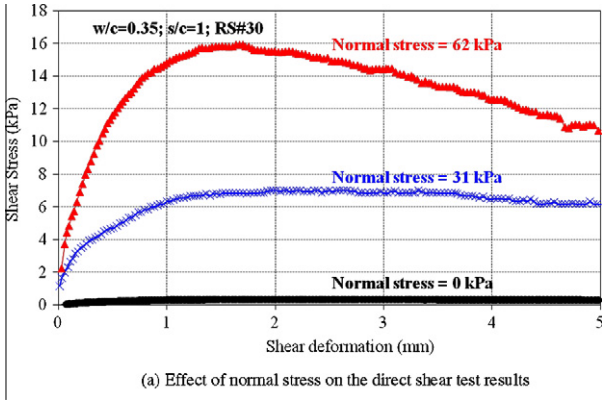

(a) Effect of normal stress on the direct shear test results

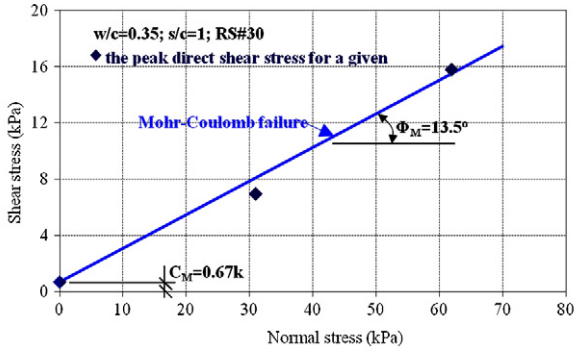

(b) Mohr-Coulomb failure curve of a mortar

Fig. 4. Typical direct shear results of a mortar sample (w/c = 0.35; s/c = 1, RS#30).

Since both Eq. (23) and the maximum shear stresses measured by the direct shear tests of a mortar under different normal stresses follow the format of the Mohr–Coulomb equation, the validity of Eq. (23) is primarily proven. Thus, the prediction of Eq. (23) can be compared with the experimental results obtained from the direct shear tests, and the parameters in Eq. (23) can also be obtained from the fitting of the test data. The features of the Mohr–Coulomb curves of the designed mortars are further discussed in the remaining parts of the paper.

4.2. Effect of cement paste rheological properties

Fig. 5 shows the Mohr–Coulomb curves of the mortar samples made with the same aggregate volume fraction (s/c = 1) and average particle size (#30) but different cement paste yield stress (τ_p): 473.6, 205.2, and 148.4 Pa (0.069, 0.030, and 0.022 psi) (w/c: 0.35, 0.40, and 0.45, correspondingly). As observed in the figure, the cohesion of a mortar (C_M) increases as the yield stress of a cement paste (τ_p) increases or the w/c of the cement paste decreases. This indicates that a larger force is required to initiate a flow for a cement paste with a higher yield stress or lower w/c, which is consistent with widely accepted knowledge [15]. However, the friction angle (ϕ_M) of the mortar has no significant change with the cement pastes. This is also consistent with Eq. (17), which indicates that the yield stress of a cement paste (τ_p) influences only the cohesion of a mortar.

4.3. Effect of aggregate content

Fig. 6 shows the Mohr–Coulomb curves for mortars made with the same cement paste (w/c = 0.45) and average aggregate size (#30) but different aggregate volume fractions (s/c = 1, 2, and 3). The Mohr–Coulomb curves of mortars show that both the cohesion (C_M) and internal friction angle (ϕ_M) of the mortar increase with

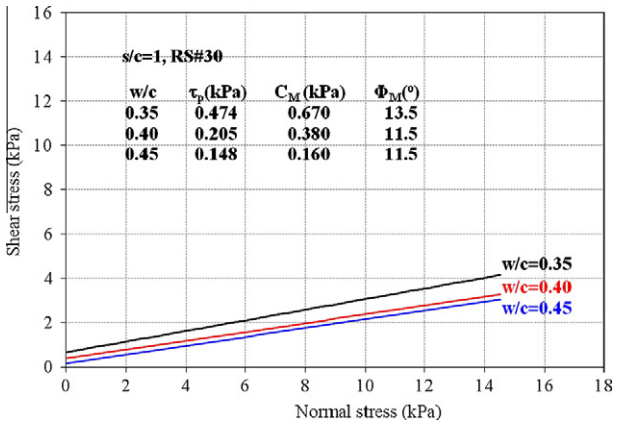

Fig. 5. Effect of cement paste on the maximum shear stress curves of a mortar.

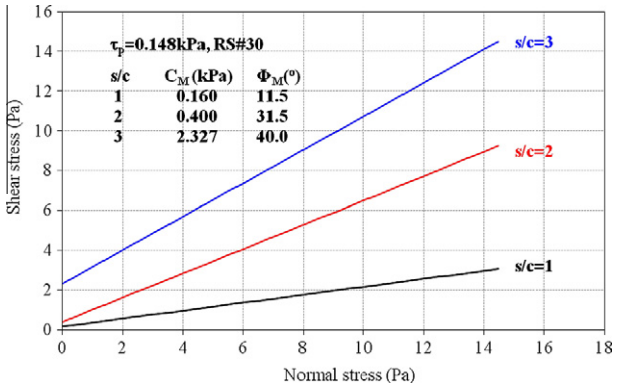

Fig. 6. Effect of aggregate content on the maximum shear stress curves of a mortar.

the increased s/c. As indicated in Eq. (6), increased aggregate volume (V_{agg}) in the mortar decreases the interparticle distance (S), which is related to the local force concentrate angle (θ) and probability parameters (P_1 and P_2). Thus, both the cohesion (C_M) and internal friction angle (ϕ_M) of the mortar are influenced as illustrated in Eqs. (20) and (21).

4.4. Effect of aggregate size

Fig. 7 shows the Mohr–Coulomb curves of the mortars made with a given paste ($w/c = 0.45$) and aggregate volume fraction ($s/c = 2$) but different aggregate sizes. Fig. 7 illustrates that the mortar made with larger aggregate has lower cohesion (C_M) and internal friction angle (ϕ_M), which suggests that the mortar has higher flowability. As indicated in Eq. (6), increased aggregate size (D_0) in the mortar increases the interparticle distance (S), which suggests that a thicker layer of cement paste is coated on the aggregate particles of the mortar, thus, increasing mortar flowability. This agrees with the common finding that a decrease in maximum size of aggregate generally increases the water demand of the concrete for the same flowability [20].

It should be mentioned that Figs. 5–7 also indicate that the normal stress has significant effect on shear resistance of mortar, especially on that of the low flowable mortar. Therefore, in a rheology test, the normal stress, which often results from the self weight of the tested material above the shear zone and the lateral confine stress from the boundary of container, should not be neglected.

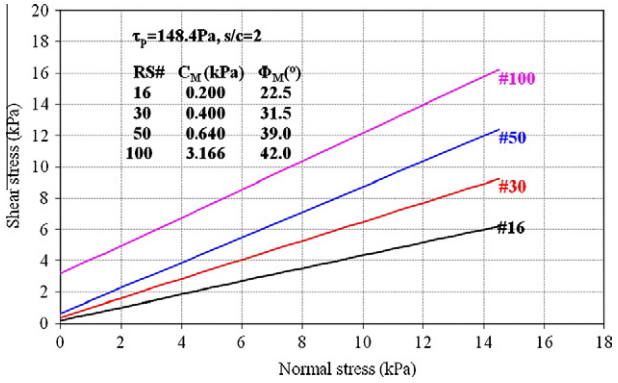

Fig. 7. Effect of aggregate size on the maximum shear stress curves of a mortar.

4.5. Effect of the average interparticle distances ($\bar{S}$) on relative shear stresses (C_M/τ_P)

As mentioned previously, the distance between aggregate particles has significant effects on the cohesion (C_M) and friction angle (ϕ_M) of the mortar. In the following two sections, these effects are investigated in detail.

Fig. 8 shows the relationship between the average interparticle distances ($\bar{S} > 0$) and the relative yield stress of mortar (C_M/τ_P), where $\bar{S}$ is calculated from Eq. (6); C_M is the shear stress of a mortar at zero normal stress, also called the cohesion or "true" yield stress of the mortar; and τ_P is yield stress of the cement paste in the mortar. It should be noted that the test data for $\bar{S} < 0$ are not included in this figure because they indicate that the volume of the cement paste in the macro-unit of mortar is not enough to fill up the voids among the aggregate particles. In this situation, the shear stress resulting from the net cement paste of the mortar (τ_{NP}) as expressed in Eq. (17) becomes negative. In an actual mortar, this shear stress (τ_{NP}) should not be negative; therefore, the mortar having an average interparticle distance $\bar{S} > 0$ is assumed and studied in the present study.

The best fitting curve of the test data presented in Fig. 8 is given as Eq. (25) ($R^2 = 0.8074$):

$$\frac{C_M}{\tau_P} = 20 \cdot e^{-0.0546*\bar{S}} + 1 \quad (R^2 = 0.8074) \tag{25}$$

where, $\bar{S}$ is in micrometer (μm).

Eq. (25) indicates that the relative yield stress (C_M/τ_P) decreases with increased average interparticle distance ($\bar{S}$) of a mortar. As illustrated in Fig. 8, when $\bar{S}$ is approximately less than 300 μm, C_M/τ_P increases very rapidly. However, when $\bar{S}$ is larger than 300 μm, C_M/τ_P is converged to 1, which suggests that the yield stress of the mortar is equal to the yield stress of the cement paste in the mortar. This research finding is valuable for concrete practice. It suggests that when a mortar (such as a self-consolidating grout) has a large average interparticle distance ($\bar{S}$), the rheological

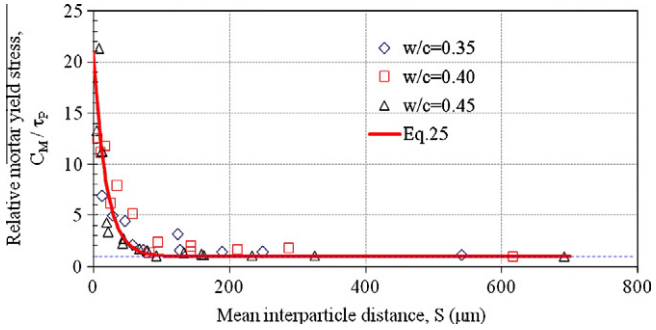

Fig. 8. Effect of the mean interparticle distance on relative yield stress of mortar.

properties of its cement paste would play a more important role in controlling the mortar flowability. For a mortar with given cement paste and aggregate size, gradation, and volume, friction can be adjusted in mix design to achieve a workable mortar or concrete.

4.6. Effect of the average interparticle distances ($\bar{S}$) on relative friction angles (ϕ_M/ϕ_{agg})

Fig. 9 shows the relationship between the average interparticle distances ($\bar{S} > 0$) and relative friction angles of mortar (ϕ_M/ϕ_{agg}), where ϕ_M and ϕ_{agg} are measured from direct shear tests. The best fitting curve of the test data is given as Eq. (26) (R^2 = 0.9505):

$$\frac{\phi_M}{\phi_{agg}} = e^{-0.005\cdot\bar{S}} + 0.1 \quad (R^2 = 0.9505) \tag{26}$$

As illustrated in Fig. 9 and Eq. (26), the relative friction angle of a mortar (ϕ_M/ϕ_{agg}) decreases steadily (in a hyperbolic logarithm form) with increased interparticle distance ($\bar{S}$) of the mortar. The influence of the interparticle distance ($\bar{S}$) on the relative mortar friction angle (ϕ_M/ϕ_{agg}) is relatively less than that on the relative mortar cohesion (C_M/τ_P).

4.7. Probability parameters and final shear stress model

Based on the discussions above, the two probability parameters, $P_1 = \frac{\tan\phi_M}{\tan\phi_{agg}}$ (Eq. (21)) and $P_2 = \frac{C_M}{\tau_P} - 1$ (Eq. (22)), should also correlate to the average interparticle distance ($\bar{S}$). Fig. 10 shows the correlation between $\frac{\tan\phi_M}{\tan\phi_{agg}}$ and average interparticle distance ($\bar{S}$). Comparing Fig. 9 and Fig. 10, it is found that the correlation between $\frac{\tan\phi_M}{\tan\phi_{agg}}$ and $\bar{S}$ is similar to that between ϕ_M/ϕ_{agg} and $\bar{S}$. Through curve fitting, similar formula as Eq. (26) can be determined for $\frac{\tan\phi_M}{\tan\phi_{agg}}$ as:

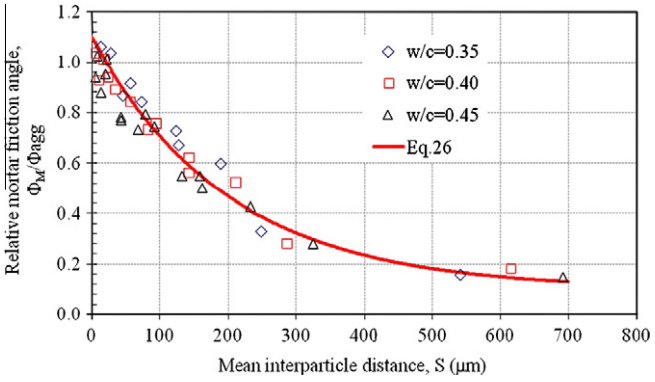

Fig. 9. Effect of the mean interparticle distance on relative friction angle of mortar.

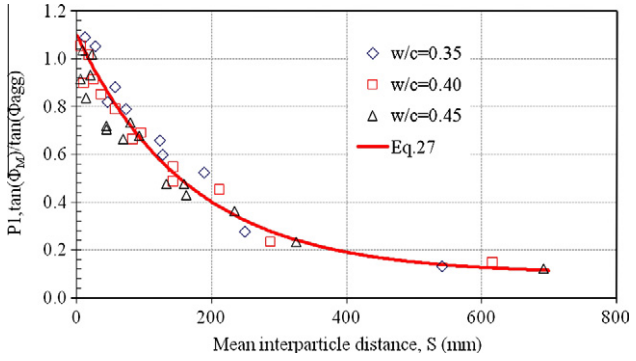

Fig. 10. Effect of the mean interparticle distance on $\frac{\tan\phi_M}{\tan\phi_{agg}}$.

$$P_1 = \frac{\tan\phi_M}{\tan\phi_{agg}} = e^{-0.006\cdot\bar{S}} + 0.1 \quad (R^2 = 0.9304) \tag{27}$$

Comparing Eq. (21) with Eq. (25), P_2 can be driven as bellows:

$$P_2 = 20\cdot e^{-0.0546*\bar{S}} \tag{28}$$

Submitting Eqs. (27) and (28) into Eq. (24), the new shear stress model for a fresh mortar can be finalized as:

$$\tau_M = (e^{-0.006\cdot\bar{S}} + 0.1)\cdot\tan\phi_{agg}\cdot\sigma + (1 + 20\cdot e^{-0.0546\cdot\bar{S}})\cdot\tau_P \tag{29}$$

Again, the average interparticle distance ($\bar{S}$) is related to aggregate size, gradation, and volume fraction and can be determined by Eq. (6); and aggregate friction angle (ϕ_{agg}) and yield stress of cement paste (τ_p) are mortar material properties and can be determined from experimental tests or other available models.

5. Conclusions

The shear behavior of fresh mortar was investigated using a force balance model and a direct shear test. The following conclusions can be made from the present investigation:

1. Both the newly developed shear stress model and the experimental results from the direct shear tests illustrate that the shear behavior of a mortar followed the Mohr–Coulomb equation. The newly developed model well simulates mortar shear behavior.
2. According to the Mohr–Coulomb equation, the internal friction angle (ϕ_M) and cohesion (C_M) of a mortar can be determined. The cohesion (C_M) of a mortar is actually the maximum shear resistance of the mortar at zero normal stress, or the "true" rheological yield stress of the mortar. Both the internal friction angle (ϕ_M) and cohesion (C_M) of a mortar greatly depend on the average interparticle distance ($\bar{S}$) of the mortar.
3. Aggregate parameters (size, gradation, and volume fraction) determine the average interparticle distance ($\bar{S}$) of a mortar, and therefore they significantly influence the shear behavior of the mortar.
4. The relative yield stress of the mortar (C_M/τ_P) decreases in an inverse power form and the relative friction angle of a mortar (ϕ_M/ϕ_{agg}) decreases in a hyperbolic logarithm form with increased interparticle distance ($\bar{S}$) of the mortar. For mortar having a large average interparticle distance ($\bar{S}$) (generally, mortar with a low aggregate volume fraction), the effects of aggregate size and gradation on the mortar yield stress appear not significant, while the effect of cement paste property becomes substantial.
5. The normal stress has significant effect on the maximum shear resistance of mortar, especially on that of the low flowable mortar. As a result, in a rheology test, the normal stress, which often results from the self weight of the tested material above the shear zone and the lateral confine stress from the boundary of container, should not be neglected.

Acknowledgments

The present study is a part of the first author's PhD dissertation. The author would like to acknowledge the National Concrete Pavement Technology Center (CP Tech Center) for support of his study through various research projects at Iowa State University.

References

[1] Peter D. Mortar test for self-consolidating concrete. Concr Inte 2006;28(4):39–45.

[2] Okamura H, Ouchi M. Self-compacting concrete. J Adv Concr Technol 2003;1(1):5–15.
[3] Saak AW, Jennings HM, Shah SP. New methodology for designing self-compacting concrete. ACI Mater J 2001;98(6):429–39.
[4] Mori H. High fluidity concrete. J Archit Build Soc 1998;113(1420):41–3.
[5] Tattersall GH, Banfill PFG. The rheology of fresh concrete. USA: Pitman Publishing Inc.; 1983.
[6] Wallevik OH, Gjørv OE. Modification of the two-point workability apparatus. Mag Concr Res 1990;42(152):135–42.
[7] Hu C, de Larrard F. The rheology of fresh high performance concrete. Cem Concr Res 1996;26(2):283–94.
[8] Li Z, Ohkubo T, Tanigawa Y. Yield model of high fluidity concrete in fresh state. J Mater Civ Eng 2004;16(3):195–201.
[9] Kennedy CT. The design of concrete mixes. Proc Am Concr Inst 1940;36:373–400.
[10] Ohea SG, Noguchi T, Tomosawa F. Toward mix design for rheology of self-compacting concrete. In: RILEM international symposium on self-compacting concrete. University of Tokyo; 1999.
[11] Smith MR, Collis L. Aggregates – sand, gravel and crushed rock aggregates for construction purposes. 3rd ed. London: The Geological Society; 2001.
[12] Struble LJ, Szecsy R, Lei W, Sun G. Rheology of cement paste and concrete. Cem, Concr, Aggr 1998;20(2):269–77.
[13] Su N, Hsu K, Chai H. A simple mix design method for self-compacting concrete. Cem Concr Res 2001;31(12):1799–807.
[14] Lu G, Wang K. Investigation into yield behavior of fresh cement paste: model and experiment. ACI Mater J 2010;107(1):12–9.
[15] Lu G, Wang K, Rudolphi TJ. Modeling rheological behavior of a highly flowable mortar using concepts of particle and fluid mechanics. Cem Concr Compos 2007;30(1):1–12.
[16] Power TC. The properties of fresh concrete. New York: John Wiley & Sons; 1968.
[17] ASTM C1252-06. The standard test method for uncompacted void content of fine aggregate, Annual Book of ASTM Standards, 04. 01; 2006.
[18] Mehrabadi MM, Nemat-Nasser S, Oda M. On statistical description of stress and fabric in granular materials. Int J Numer Anal Methods Geomech 1982;6(1):95–108.
[19] ASTM C305-99. Standard practice for mechanical mixing of hydraulic cement pastes and mortars of plastic consistency, Annual Book of ASTM Standards, 04. 01; 2003.
[20] Mehta PK, Monteiro PJM. Concrete-structure, properties and materials. 2nd ed. Prentice Hall; 1993.